Molecular Basis of TCR Selectivity, Cross-Reactivity, and Allelic Discrimination by a Bacterial Superantigen: Integrative Functional and Energetic Mapping of the SpeC-Vβ2.1 Molecular Interface[1]

A. K. M. Nur-ur Rahman,*†‡ Christine A. Herfst,*†‡ Beenu Moza,¶ Stephanie R. Shames,*†‡ Luan A. Chau,§ Clara Bueno,[2]§ Joaquín Madrenas,†§ Eric J. Sundberg,¶ and John K. McCormick[3]*†‡

Superantigens activate large fractions of T cells through unconventional interactions with both TCR β-chain V domains (Vβs) and MHC class II molecules. The bacterial superantigen streptococcal pyrogenic exotoxin C (SpeC) primarily stimulates human Vβ2$^+$ T cells. Herein, we have analyzed the SpeC-Vβ2.1 interaction by mutating all SpeC residues that make contact with Vβ2.1 and have determined the energetic and functional consequences of these mutations. Our comprehensive approach, including mutagenesis, functional readouts from both bulk T cell populations, and an engineered Vβ2.1$^+$ Jurkat T cell, as well as surface plasmon resonance binding analysis, has defined the SpeC "functional epitope" for TCR engagement. Although only two SpeC residues (Tyr^{15} and Arg^{181}) are critical for activation of virtually all human CD3$^+$ T cells, a larger cluster of four hot spot residues are required for interaction with Vβ2.1. Three of these residues (Tyr^{15}, Phe^{75}, and Arg^{181}) concentrate their binding energy on the CDR2 loop residue Ser^{52a}, a noncanonical residue insertion found only in Vβ2 and Vβ4 chains. Plasticity of this loop is important for recognition by SpeC. Although SpeC interacts with the Vβ2.1 hypervariable CDR3 loop, our data indicate these contacts have little to no influence on the functional interaction with Vβ2.1. These studies also provide a molecular basis for selectivity and cross-reactivity of SpeC-TCR recognition and reveal a degree of fine specificity in these interactions, whereby certain SpeC mutants are capable of distinguishing between different alleles of the same Vβ domain subfamily. *The Journal of Immunology,* **2006, 177: 8595–8603.**

Superantigens (SAgs)[4] are potent immunostimulatory molecules of microbial origin that function to activate large proportions of T cells by binding as intact proteins to MHC class II molecules on APCs, and TCRs on T cells, through unconventional surfaces. These interactions displace the TCR away from MHC class II such that SAg-mediated T cell activation occurs independent of the antigenic peptide loaded into the MHC class II molecule (1–7). The $\alpha\beta$ TCR is targeted by SAgs through the V domain of the β-chain (termed Vβ), which subsequently leads to the activation of T cells in a Vβ-specific manner (8). In humans, the number of functional TCR Vβ gene segments is limited to ~50, comprising 26 major classes of β-chains in the TCR repertoire (9, 10). Because SAgs may bind to more than one Vβ chain, large numbers of T cells can be activated (up to 20%), and it is this hyperactivation, with the accompanying release of massive amounts of cytokines, that is believed to result in toxic shock syndrome (11). Due to the potential activation and proliferation of autoreactive T cells, SAgs may also be involved in some autoimmune diseases (12). Following their initial expansion, the majority of the T cells die by apoptosis and a minority survive in anergized form (13).

Based on the crystal structures solved for TCR-SAg and SAg-peptide-MHC (SAg-p/MHC) complexes, trimolecular (TCR-SAg-p/MHC) complexes have been modeled. In the first model represented by staphylococcal enterotoxin (SE) B, SEC3, and likely streptococcal pyrogenic exotoxin (Spe) A, the SAg acts as a "wedge" between the TCR and p/MHC molecules which displaces the TCR β-chain away from interacting with the MHC class II α-chain, while permitting nonconventional interactions between the TCR α-chain and the MHC β-chain (14). Biochemical studies have confirmed that the interaction between the CDR2 loop of the TCR α-chain and the MHC class II β-chain stabilizes the trimolecular structure (15), resulting in an energetically cooperative TCR-SAg-p/MHC supramolecular complex that exhibits an affinity similar to that of most agonist p/MHC interactions with TCR (16). In a second model, represented by SpeC, the SAg acts as a "bridge", which abrogates any direct contacts between the TCR

*Lawson Health Research Institute, †Department of Microbiology and Immunology, and ‡Bacterial Pathogenesis Research Group, University of Western Ontario, and §The FOCIS Centre for Clinical Immunology and Immunotherapeutics and Robarts Research Institute, London, Ontario, Canada; and ¶Boston Biomedical Research Institute, Watertown, MA 02472

Received for publication April 27, 2006. Accepted for publication September 29, 2006.

The costs of publication of this article were defrayed in part by the payment of page charges. This article must therefore be hereby marked *advertisement* in accordance with 18 U.S.C. Section 1734 solely to indicate this fact.

[1] This work was supported by Canadian Institutes of Health Research (CIHR) operating grants (to J.K.M. and J.M.) and National Institutes of Health Grant AI55882 (to E.J.S.). C.B. was supported by a fellowship from the Ontario Research and Development Fund, J.M. holds a Canada Research Chair in Transplantation and Immunobiology, and J.K.M. holds a New Investigator award from the CIHR.

[2] Current address: Section of Haemato-Oncology, The Institute of Cancer Research, Chester Beatty Laboratories, 237 Fulham Road SW3 6JB, London, U.K.

[3] Address correspondence and reprint requests to Dr. John K. McCormick, Department of Microbiology and Immunology, University of Western Ontario, London, Ontario, Canada N6A 5C1. E-mail address: john.mccormick@schulich.uwo.ca

[4] Abbreviations used in this paper: SAg, superantigen; p/MHC, peptide-MHC; SE, staphylococcal enterotoxin; Spe, streptococcal pyrogenic exotoxin; HV, hypervariable region; FR, framework region; SPR, surface plasmon resonance; TEV, tobacco etch virus.

0022-1767/06/$02.00

and p/MHC molecules (1). In this complex, the higher affinity interaction between SpeC and p/MHC (5) is believed to stabilize the trimolecular complex.

Recent bacterial genome sequencing projects have revealed a large number of genetically distinct SAgs present in pathogenic *Staphylococcus aureus* and *Streptococcus pyogenes*. These SAgs belong to the pyrogenic toxin class of SAgs (11) and currently there are >30 identified serotypes (17). Even though most of these toxins share relatively low amino acid sequence identity, all characterized SAgs from this class have a conserved two-domain structure including a smaller N-terminal domain and a larger C-terminal domain with a central α helix connecting the two domains (18). Despite their similar structures, SAgs display diversity in binding to their TCR ligands as revealed by a limited number of SAg-TCR crystal structures. Atomic structures of SEB (6), SEC3 (14), and SpeA (1) have been characterized with a single TCR β-chain, mouse Vβ8.2, and the SpeC structure has been solved in complex with the human TCR β-chain Vβ2.1 (1). In each case, the SAg binds to TCR molecules with residues positioned in the cleft between the two SAg domains, yet the structure of Vβ2.1 in complex with SpeC revealed considerable binding differences compared with other SAg-β-chain complexes. SpeC makes multiple contacts with both side chain and main chain atoms of Vβ2.1, and was unique among characterized SAg-TCR interactions in that all three CDR loops were engaged, as well as the hypervariable (HV) region 4 and framework region (FR) 3 (1). In particular, the CDR3 contacts were unexpected because this loop is highly variable even within a single Vβ family due to somatic recombination. Also, the buried surface of the SpeC-Vβ2.1 is comparable to that of TCR-p/MHC complexes, considerably larger than the contact surfaces for other SAg-TCR complexes (1, 6, 14). However, the molecular basis by which particular SAgs bind to certain TCR Vβ domains but not to others, as well as why some SAgs are highly restrictive in their Vβ-binding partners while others are promiscuous binders, is presently unclear.

The SpeC-Vβ2.1 crystal structure (1) identified all of the intermolecular contacts that form the interface of this complex (the "structural epitope"). Structural studies alone, however, cannot provide a comprehensive understanding of the molecular basis for complex formation, because protein-protein interactions are not homogenous energetic landscapes. Instead, hot spot residues, which confer the majority of the binding energy to a given complex (the "functional epitope"), are interspersed with energetically silent residues (19–21). Algorithms developed to predict the energetic contribution of individual residues (22–26), while greatly advanced in the past few years, do not provide accurate enough predictions to alleviate the current need to determine these values experimentally. Furthermore, protein complexes function in the context of larger biological systems, and thus, the structural and energetic dissection of a protein-protein interaction can provide a truly comprehensive understanding of the complex only when integrated with functional analysis.

To provide such a comprehensive understanding of Vβ2.1 engagement by SpeC, we have mutated every SpeC residue involved in the SpeC-Vβ2.1 molecular interface to alanine. We determined the binding affinities of these mutants and wild type SpeC to soluble Vβ2.1 by surface plasmon resonance (SPR) analysis, as well as their functional readouts upon stimulation of both bulk T cells and an engineered Vβ2.1$^+$ T cell line. Collectively, our energetic and functional data define the functional epitope on the SpeC molecular surface and provide the molecular basis for SpeC-TCR Vβ domain selectivity, cross-reactivity, and allelic discrimination.

Materials and Methods

Cloning procedures

Standard DNA manipulations were performed as described (27) using enzymes supplied from New England Biolabs in accordance with the manufacturer's instructions. Oligonucleotides were obtained from Invitrogen Life Technologies. PCRs were performed in a Peltier Thermocycler (MJ Research) with *Vent* DNA polymerase (Invitrogen Life Technologies) and PCR products were purified using the QIAquick PCR purification kit (Qiagen). All cloned PCR products were sequenced in their entirety at the John P. Robarts Research Institute Sequencing Facility (London, Ontario, Canada) to ensure correct mutations and PCR fidelity. *Escherichia coli* was cultured aerobically in Luria Bertani broth (Difco Laboratories) at 37°C, and solid medium was obtained by the addition of 1.5% (w/v) Bacto-agar (Difco). Kanamycin (50 μg/ml) and ampicillin (100 μg/ml) were used as selective agents as required. All reagents were made with water purified through a Milli-Q water purification system (Millipore).

SpeC mutants

For expression of the various SpeC proteins, we first generated a modified version of the *E. coli* expression vector pET41a (Novagen). Overlapping complementary primers were designed (5′-CGGTGGTGGCTCCGGT GAAAACTTGTATTTCCAAGGCAGTCC-3′ and 5′-CATGGGACTGC CTTGGAAATACAAGTTTTCACCGGAGCCACCACCGGTAC-3′) that when annealed leave overhangs compatible with the *Kpn*I and *Nco*I sites of pET41a. When ligated into these sites (to create pET41a::TEV), the pET41a enterokinase cleavage site (DDDDK) is replace with the tobacco etch virus (TEV) protease cleavage site (ENLYFQG) (28) leaving other features of the plasmid intact. Wild-type *speC* was PCR amplified from pET28a::*speC* (29) with primers SpeC-forward (5′-CCCATGGCAG ACTCTAAGAAAGACATTTCGAATG-3′; *Nco*I site underlined) and SpeC-reverse (5′-CCCGGATCCTTATTTTTCAAGATAAATATCGAA ATG-3′; *Bam*HI site underlined) where the forward primer amplified *speC* lacking the coding region for the 27-aa signal peptide (30). The resulting PCR product was cloned into pET41a::TEV creating an N-terminal translational fusion of GST and His_6 purification tags with SpeC, as well as the TEV site for removal of the purification tags. The various SpeC mutant proteins were generated using an overlapping megaprimer PCR method using oligonucleotides that incorporated the desired single-site mutation. SpeC proteins were expressed from *E. coli* BL21(DE3) (Novagen), purified by Ni^{2+}-column chromatography, and the purification tags were removed with autoinactivation-resistant His_7::TEV as described (28).

LG-2 aggregation assay

The B lymphoid cell line LG-2 was used in cell aggregation experiments (31) and was performed with all the SpeC mutant proteins as an indication of overall protein conformation and to assess the ability of the mutants to engage MHC class II. LG-2 cells (100,000 cell/ml) suspended in RPMI 1640 (Invitrogen Life Technologies) supplemented with 10% FCS (Sigma-Aldrich), 100 μg/ml streptomycin (HyClone), 100 U/ml penicillin (HyClone), 2 mM L-glutamine (HyClone), 1 mM MEM sodium pyruvate (HyClone), 100 μM nonessential amino acid (HyClone), and 25 mM HEPES (pH 7.2) (BioShop) were plated into each well of a 96-well plate. Afterward, 1 μg of each protein was added and aggregation was monitored under an inverted microscope at various time points.

PBL proliferation measurements

The studies were reviewed and approved by University of Western Ontario Research Ethics Board for Health Sciences Research Involving Human Subjects. The ability of purified recombinant wild-type and mutant SpeC proteins to proliferate human T cells was assessed using gradient-purified human PBMCs stimulated ex vivo in 96-well microtiter plates (2×10^5 cells/well) with serial 1/5 dilutions (in triplicate). RPMI 1640 medium supplemented as above for the LG-2 assays was used as the culture medium and cells were incubated in 5% CO_2 at 37°C. Cells were pulsed with 1 μCi/well [^{3}H]thymidine after 72 h and after another 18 h cells were harvested on fiberglass filters and [^{3}H]thymidine incorporation was assessed on a 1450 Microbeta liquid scintillation counter (Wallac). Background was considered as counts from cells not treated with toxin.

Flow cytometry of activated Vβ2$^+$ T cells

SpeC has been previously shown to activate T cells expressing Vβ2$^+$ TCRs (31). To specifically examine the relative contribution of each mutant for activation of Vβ2$^+$ T cells, expression of CD3, Vβ2, and CD25 was analyzed in a FACSCalibur flow cytometer (BD Biosciences) with PBMCs (1×10^6/ml) activated with 1 ng/ml of the various SpeC mutants

Table I. *Functional characteristics of the SpeC mutants*[a]

SpeC Protein	*Mitogenic Capacity* (pg/ml)[b]	Affinity Measurements		T Cell Activation	
		K_D BIAcore ($\times 10^{-6}$ *M*)[c]	$\Delta\Delta G_b$ (kcal/mol)[d]	Vβ2$^+$ primary T cells	Vβ2.1 Jurkat T cells
Wild-type	273	13	−	+	+
Y15A	>500,000	NB	>1.20	−	−
T18A	601	32	0.53	+	+
I19A	1,062	NB	>1.20	+	+
T20A	532	9	−0.22	+	+
R45A	219	14	0.04	+	+
Y49A	1,258	15	0.10	+	+
F75A	1,490	NB	>1.20	+	−
L78A	2,854	NB	>1.20	+	−
N79A	1,155	30	0.49	+	+
E178A	777	NB	>1.20	+	+
T180A	1,139	15	0.08	+	+
R181A	>500,000	NB	>1.20	−	−

[a] Mitogenic capacity of SpeC mutants for primary human T cells, dissociation constants for binding of SpeC mutants to rVβ2.1, and summary of T cell activation measurements for Vβ2$^+$ primary T cells and Vβ2.1-specific Jurkat T cells.

[b] Mitogenic capacity of the SpeC molecules was calculated by the dose (picograms per milliliter) required to induce 50% of the mitogenic activity compared with maximal activity of wild-type SpeC. Data are averages of experiment done at least twice in triplicate.

[c] NB, No binding detected up to 100 μM Vβ2.1.

[d] ΔG_b was calculated according to the equation $\Delta G_b = -RT \ln (1/K_D)$, where R is the universal gas constant and T is the absolute temperature in Kelvin. $\Delta\Delta G_b = \Delta G_{b\ mutant} - \Delta G_{b\ wild\ type}$.

for 3 days. Data analysis was performed with FlowJo software. The mAbs used were: FITC-labeled anti-Vβ2 (Immunotech; Beckman Coulter), PE-labeled anti-CD25 (BD Biosciences/BD Pharmingen) and PC5-labeled anti-CD3 Ab (Immunotech/Beckman Coulter).

Surface plasmon resonance

Vβ2.1Dβ2.1Jβ2.3Cβ2 (herein referred to as Vβ2.1) was expressed, refolded, and purified as previously described (1). Binding affinities of Vβ2.1 to immobilized SpeC and the various mutants were monitored with a BIAcore 3000 instrument (Biacore). SAgs were coupled via amine groups to a dextran matrix on CM5 sensor chips, at a total mass corresponding to ~500 resonance units. SEB, in an equivalent surface density, was used as a negative control surface, as no specific binding of the Vβ2.1 chain to this SAg occurs. Vβ2.1 was dialyzed against 10 mM Na-HEPES (pH 7.5), 150 mM NaCl, 3.4 mM EDTA, 0.005% P20 surfactant (HBS-P20) and was characterized immediately before injection by size exclusion chromatography to ensure that no aggregation was present. Measurements were conducted at 25°C by injecting increasing concentrations of Vβ2.1 up to a maximum of 100 μM at a flow rate of 10 μl/min. Affinities (K_D) were determined by nonlinear regression analysis of equilibrium binding from multiple concentrations of injected Vβ2.1 using BIAevaluation 4.1 software (Biacore).

Construction of Vβ2.1 expressing Jurkat T cells and activation measurements

To allow for a functional readout for the SpeC mutants specific for the Vβ2.1 chain used in the SpeC-Vβ2.1 complex (1), the Jurkat T cell line JRT3-T3.5 (American Type Culture Collection) was used. This cell line lacks the endogenous Vβ8.1 chain present in wild-type Jurkat T cells (32). The leader and transmembrane DNA sequences of human Vβ8.1 (33) were attached to the 5′ and 3′ ends of Vβ2.1 cDNA, respectively, to promote surface expression and successful pairing of Vβ2.1 with the endogenous Vα1. In addition, alanines at positions 13 and 191 generated for the cocrystal structure with SpeC (1) were back-mutated to the native cysteine residues. All of these modifications to the Vβ2.1 cDNA were performed by sequential megaprimer PCR and the complete Vβ2.1 cDNA was cloned into the unique *Kpn*I and *Bam*HI sites in pBIG2i (34). This vector has an ampicillin-resistant marker for cloning purposes in *E. coli*, a hygromycin B-resistant marker for establishing stable cell lines and a tetracycline responsive system for the induction of the desired gene. Ten micrograms of linearized pBIG2i::Vβ2.1 was electroporated into 5,000,000 JRT3-T3.5 cells using 300 V and 950 μF and stable transfectants were selected using increasing concentrations of hygromycin B. JRT3-T3.5 transfected with pBIG2i alone was used as a negative control. Surface expression of Vβ2.1 paired with endogenous Vα1 was induced with doxycycline at a concentration of 1 μg/ml and surface expression was confirmed using FACS analysis with PE-conjugated anti-TCR Ab (eBioscience). Further verification of the expressed TCR was performed with FITC-conjugated anti-Vβ2 Ab. Transfected JRT3-T3.5 were incubated with LG-2 cells (in 5:1 ratio) to provide MHC class II (HLA-DR1) in the presence of SpeC proteins (1 ng/ml) for 16–18 h. Activation was monitored using ELISA for IL-2.

Results

SpeC mutants

The crystal structure of the SpeC-Vβ2.1 complex revealed that 12 residues of SpeC collectively make up the structural epitope for binding to Vβ2.1. To define the SpeC functional epitope, we performed alanine-scanning mutagenesis analysis for all SpeC residues in contact with Vβ2.1. Alanine was chosen as the mutating residue to replace the side chains of the interacting residues because of its inherent attribute to minimize steric or electrostatic constrains on the tertiary structure of the protein (35). All SpeC proteins were expressed from *E. coli* BL21(DE3) and purified to apparent homogeneity as determined by SDS-PAGE (data not shown). As SpeC is known to aggregate the B lymphoblastoid LG-2 cell line through the cross-linking of MHC class II molecules expressed on these cells (31), we used this assay to confirm the point mutations did not cause gross structural defects in the mutant proteins. Each of the mutant proteins was able to aggregate LG-2 cells as expected, while a negative control SAg (SpeA) did not cause aggregation (data not shown). In addition, circular dichroism analysis confirmed that the point mutations did not induce any gross structural deviations in the proteins (data not shown).

Proliferation of human T cells by SpeC mutants

We examined the ability of each mutant to proliferate human PBMCs using standard [^{3}H]thymidine assays. The stimulatory capacity (P_{50}) is defined as the concentration of SpeC mutant protein required to reach 50% of the maximum proliferation relative to wild-type SpeC. SpeC mutants produced dose-dependent proliferation curves, whereas wild-type reached P_{50} at ~0.273 ng/ml (Table I). Wild-type SpeC typically reached a maximum plateau by ~4 ng/ml and then decreased as the concentration increased to the highest concentration tested (500 ng/ml). Of the 12 mutants, two mutants (Y15A and R181A) showed a dramatic decrease in activity and did not reach the P_{50} value even at concentrations of 500 ng/ml. Based on P_{50} values,

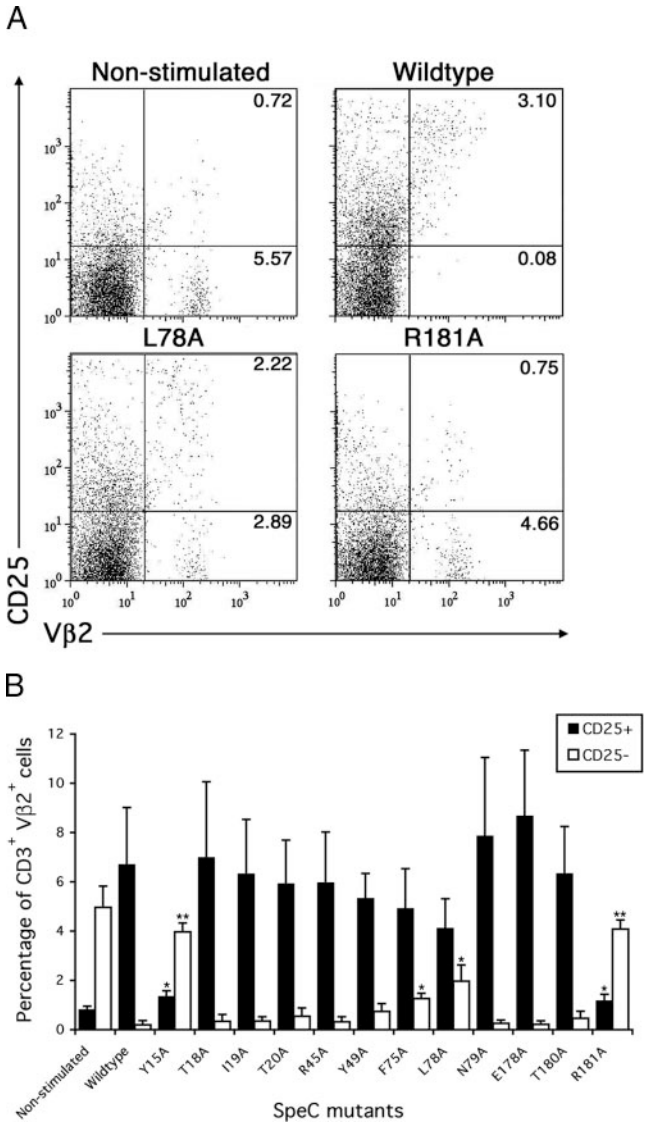

FIGURE 1. Vβ2-specific activation of PBLs by the alanine-substituted SpeC mutants. *A*, Representative flow cytometry plots of human PBMCs (1×10^6/ml) activated with 1 ng/ml of the various SpeC mutants for 3 days. $CD3^+$ cells were analyzed for expression of both Vβ2 and CD25. Plots are representative experiments from a single donor. *B*, Quantitation of activated ($CD25^+$) or nonactivated ($CD25^-$) $V\beta2^+CD3^+$ T cells. Data shown are the average ± SEM from three independent experiments, each with a different donor (*, $p < 0.05$; **, $p < 0.01$ compared with wild-type SpeC).

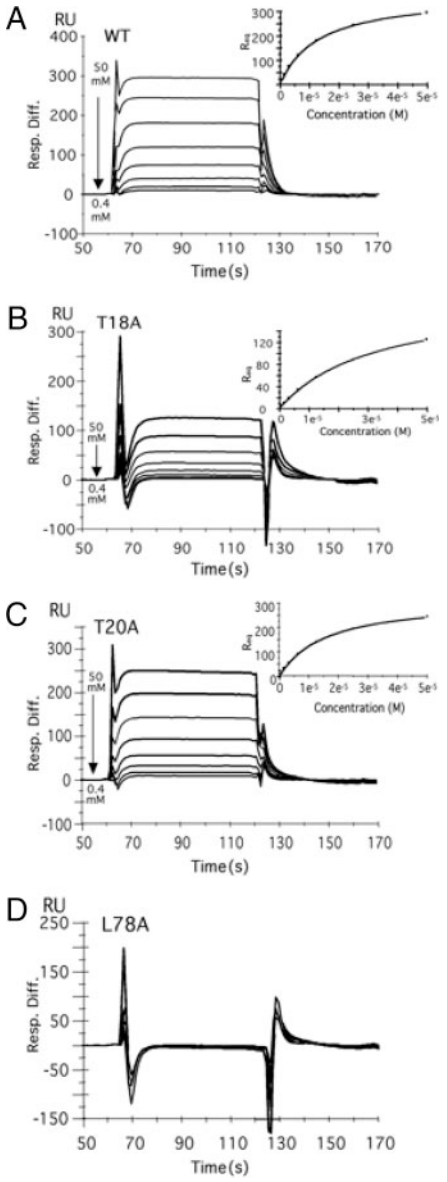

FIGURE 2. Characterization of the alanine-substituted SpeC mutants for binding to soluble Vβ2.1 by surface plasmon resonance (SPR). Sensorgrams are representative of decreased binding affinity (T18A) (*B*), no effect on binding (T20A) (*C*), and no binding (L78A) (*D*) as compared with wild-type Vβ2.1 (WT) (*A*). *Inset* (in *A–C*), Nonlinear steady state analysis of each interaction.

most of the other SpeC mutants showed minor reductions in activity relative to wild type, with the greatest loss of activity occurring with L78A, F75A, and Y49A mutants (~11-, 6-, and 5-fold reductions, respectively) (Table I).

Activation of $V\beta2^+$ T cells by SpeC mutants

Because the majority of SpeC-targeted T cells are represented by $V\beta2^+$ T cells (31) and the alanine-scanning mutants were based on the cocrystal structure with Vβ2.1 (1), we evaluated the effect of the SpeC mutants on $V\beta2^+$ T cells. We monitored activation of $CD3^+V\beta2^+$ T cells from human PBMCs using the up-regulation of CD25 as a measure of Vβ2-specific T cell activation. CD25 is the α-chain of the high-affinity IL-2R which is up-regulated upon T cell activation and is a member of the early response gene family of naive T cells. CD25 expression gradually increases to maximum levels by day 3 after stimulation and afterward the expression level is maintained on T cells (36). Approximately 7% of total T cells from a healthy donor are $V\beta2^+$ and roughly 1% of these $V\beta2^+$ T cells were routinely found $CD25^+$ in the absence of stimulation (Fig. 1). Upon stimulation with wild-type SpeC, however, the percentage of activated $V\beta2^+$ T cells, as monitored by the up-regulation of CD25, increased to ~7% of total T cell population with virtually no resting cells, indicating that essentially all $V\beta2^+$ T cells present in the population were activated. There was also a marked increase in the percentage of activated T cells that were not $V\beta2^+$ (Fig. 1*A*), and these populations likely represent other SpeC-targeted Vβs. The majority of $V\beta2^-$ cells, marked by the absence of CD25, though, were not activated by SpeC, as expected.

The activation profiles for the Y15A and R181A mutants were similar to untreated cells indicating that these mutants were drastically impaired (Fig. 1*B*). The activation profile for F75A and

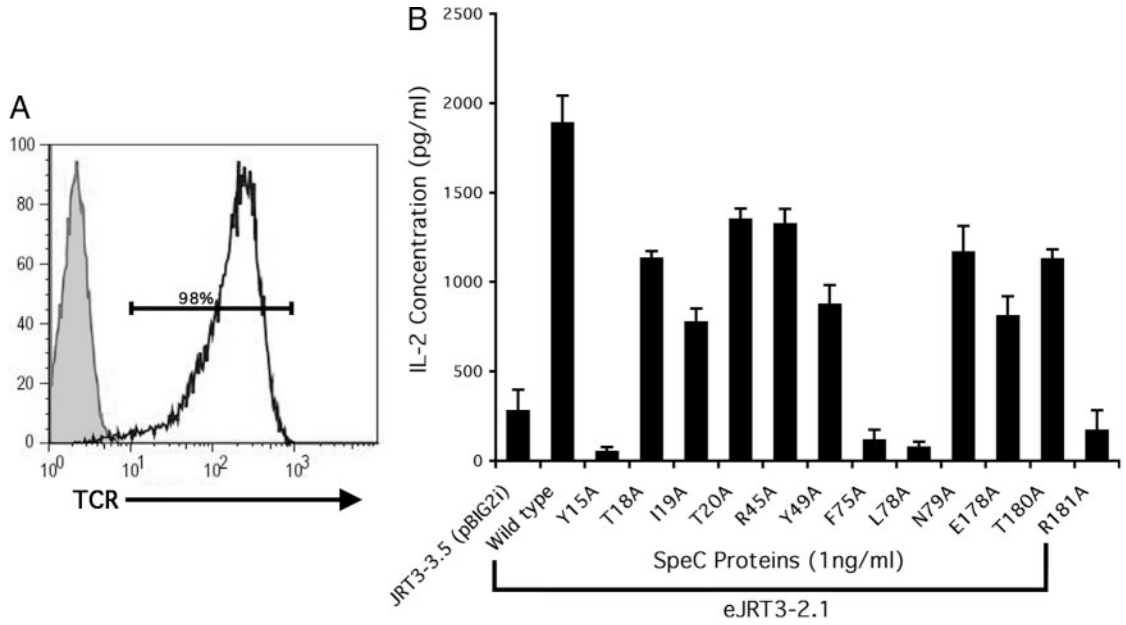

FIGURE 3. Reconstitution of the Vβ2.1/Vα1 TCR in Jurkat T cells and activation by the alanine-substituted SpeC mutants. *A*, Demonstration of TCR expression in JRT3-T3.5 stably transfected with pBIG2i::Vβ2.1 as described in *Materials and Methods*. Cells were stained with PE-labeled anti-TCR Ab (black line) or isotype control (gray shading). *B*, IL-2 secretion by eJRT3-2.1 cells incubated with 1 ng/ml of the SpeC mutant proteins in the presence of LG-2 cells. Data shown are the average ± SEM of two independent experiments, each done in triplicate.

L78A mutants, consistent with their P_{50} values for the complete T cell repertoire (Table I), were also reduced (Fig. 1*B*). In contrast, most of the other SpeC mutants did not markedly differ from wild type. Also of note, both the F75A and L78A mutants failed to stimulate a significant subpopulation (1.5–2%) of Vβ2$^+$ T cells that were activated by wild-type SpeC (Fig. 1). Thus, specific mutations in SpeC appear to allow for the discrimination of different alleles within a specific Vβ family.

Direct binding of Vβ2.1 to SpeC mutants

To examine the interaction between the various SpeC mutants and the Vβ2.1 allele used in the cocrystal structure (1), we determined the binding affinity of each mutant to Vβ2.1 by SPR (Table I). Representative profiles of equilibrium binding between immobilized wild-type and mutant SpeC proteins and Vβ2.1 and their corresponding nonlinear regression analyses of binding are shown in Fig. 2. The K_D values and differences in the changes in binding free energy relative to wild type ($\Delta\Delta G_b$) of all of the interactions are listed in Table I. None of the mutants bound Vβ2.1 with significantly higher affinity than did wild-type SpeC (K_D = 13 μM).

This binding analysis between the SpeC mutants and Vβ2.1 provides the energetic contribution of individual residues in stabilizing the SpeC-Vβ2.1 complex. Energetically, the SpeC mutants can be divided into three groups: 1) neutral mutants (T20A, R45A, Y49A, and T180A) that had no significant change on the overall binding; 2) intermediate mutants (T18A and N79A) that decreased the binding affinity of SpeC for Vβ2.1 by approximately half; and 3) critical mutants (Y15A, I19A, F75A, L78A, E178A, and R181A) that abrogated any detectable binding up to 100 μM Vβ2.1 (~10-fold lower concentration than the wild-type SpeC-Vβ2.1 K_D). This data indicates that although the binding site for Vβ2.1 on the SpeC molecular surface is quite large, only a specific subset of SpeC residues is important for complex formation.

Derivation of a Vβ2.1-specific functional readout

To better identify the functional epitope on SpeC, to mimic physiological conditions as closely as possible, and to determine whether the energetic contributions of the residues can be correlated to their functional contributions, we engineered the non-TCR-expressing Jurkat T cell line JRT3-T3.5 to exclusively express the Vβ2.1 chain. The normal $\alpha\beta$ TCR on Jurkat T cells is comprised of the Vβ8.1 chain conjugated to the Vα1 chain. However, in JRT3-T3.5, the *Vβ8.1* gene is defective, rendering it unable to express the paired $\alpha\beta$ TCR on the surface. Our engineered JRT3-T3.5 (eJRT3-2.1) cell line expresses the Vβ2.1 chain paired with the endogenous Vα1 (data not shown). Even in the absence of the inducer doxycycline and under our conditions, we achieved almost 100% expression of the TCR (Fig. 3*A*), and thus, we conducted all experiments without induction.

The eJRT3-2.1 cells were incubated with LG-2 cells (which provide a source of MHC class II molecules) in the presence of either wild-type SpeC or the individual alanine mutants. Activation was assessed by measuring IL-2 secretion by ELISA (Fig. 3*B*) and IL-2 expression profiles correlated to the measured affinities of the SpeC proteins. Wild-type SpeC proteins induced the highest IL-2 secretion levels by the eJRT3-2.1 cells, whereas the neutral and intermediate mutants induced similar levels of IL-2 secretion, even though the intermediate mutants exhibit affinities for Vβ2.1 that are ~2-fold weaker. Four of the mutants (Y15A, F75A, L78A, and R181A) with no detectable binding to soluble Vβ2.1 did not produce significant levels of IL-2 from eJRT3-2.1 cells. However, for the I19A and E178A mutants, which also lacked detectable binding to soluble Vβ2.1 (up to 100 μM), only reduced quantities of IL-2 were secreted.

Discussion

Bacterial SAgs represent a unique class of microbial toxin that has evolved to target two key immune cell receptors, the TCR and MHC class II. The collective family of bacterial SAgs includes over 30 recognized serotypes (17), which now greatly exceeds those that have been structurally characterized with their TCR and MHC ligands. Although there exists a high degree of structural

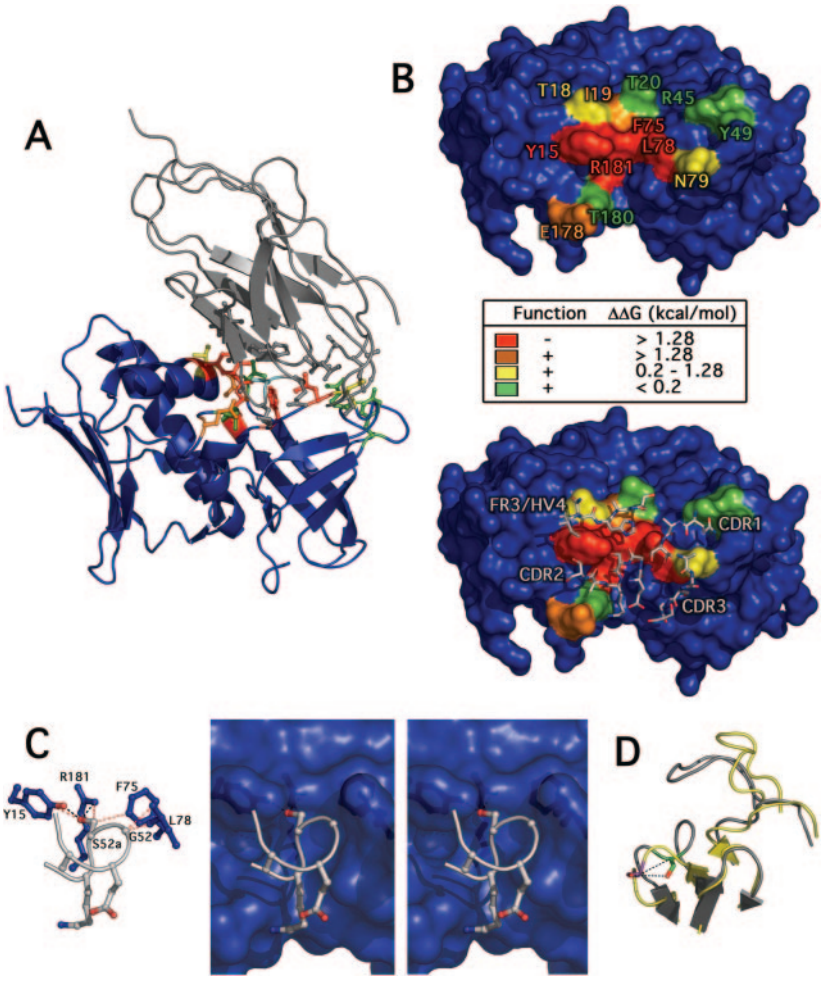

FIGURE 4. Overview of the SpeC functional epitope for interaction with Vβ2.1. *A*, Ribbon diagrams showing the interaction of Vβ2.1 (gray) and SpeC (blue) from the cocrystal structure (1). The TCR Cβ is omitted for clarity. Side chains making intermolecular contacts are shown. *B*, Surface representation of the SpeC functional epitope for interaction with Vβ2.1 viewed from the perspective of the TCR. Mutated residues that were functionally critical for the interaction with Vβ2.1 are shown in red, those that remained functional but lacked detectable binding are shown in orange, residues that demonstrated minor reductions in binding are shown in yellow, and residues with little to no effect on the interaction are shown in green. Residues are labeled in the *top panel* and the locations of the CDR loops are shown in the *bottom panel*. The color scale summarizes the functional and energetic consequences of mutating each residue to alanine. *C*, Close-up view of the four critical residues that surround the Ser^{52a} noncanonical residue insertion in the CDR2 loop of Vβ2.1. Relevant residues are labeled in the *left panel* where black lines represent hydrogen bonds and red lines represent van der Waals interactions. The *right panels* show a stereo view of the insertion of CDR2 loop Ser^{52a} into the hot region of SpeC, shown as a transparent surface with the key side chains shown as stick representations. *D*, Superimposition of two independent Vβ2.1 alleles showing the CDR 1, 2, and 3 loops, as well as FR3/HV4. Shown in gray is the Vβ2.1 allele from the SpeC-Vβ2.1 cocrystal (1) with the Ser^{52a} side chain colored green, and shown in yellow is the Vβ2.1 allele from an autoimmune TCR-peptide-MHC complex with the Ser^{52a} side chain colored purple (42). Dashed lines illustrate the movement of Ser^{52a} demonstrating the altered conformation of the CDR2 loop between the two structures.

homology between these SAgs, dramatically distinct molecular architectures of the ternary TCR-SAg-p/MHC T cell signaling complexes can be formed. The most significant factor in supramolecular architecture diversity is the numerous ways in which SAgs interact with their MHC ligands. The ways in which SAgs recognize their TCR ligands, although not as radically diverse as SAg-p/MHC interactions, are also varied. This is the determining factor for which distinct subsets of T cells are activated by individual SAgs.

The crystal structure of SpeC in complex with Vβ2.1 revealed that SpeC contacts included all three Vβ CDR loops, as well as FR2 and FR3/HV4 regions, and consequently the buried interface was much larger than other characterized SAg-TCR complexes, being more similar in size to typical TCR-p/MHC complexes (1). The binding characteristics of SpeC to Vβ2.1 also led to the suggestion that SAgs may target their TCRs in at least three distinct ways (37). One group, represented by SEB and SEC3, which would be highly promiscuous for T cell activation, target Vβs mainly on a conformational basis, making only contacts with Vβ main chain atoms. A second group, represented by SpeA, targets both Vβ main chain and side contacts, and would be more selective. The third group, represented by SpeC, targets only Vβ amino acid side chains, and would therefore be highly selective. Despite these multiple modes for activation of T cells, each is capable of generating a highly Vβ-skewed population of T cells. This rudimentary classification of SAg-TCR recognition is severely limited by the paucity of SAg-TCR crystal structures, which are currently restricted to SEB, SEC3, and SpeA bound to mouse Vβ8.2 (1, 6, 14) and SpeC bound to human Vβ2.1 (1). Thus, our understanding of how each distinct SAg recognizes its particular subset of TCR Vβ domain ligands, and the molecular basis of SAg-TCR specificity and cross-reactivity, remain unclear.

Although the cocrystal structure of SpeC in complex with human Vβ2.1 has provided a molecular snapshot of all contacts within this interface (1) (Fig. 4*A*), it does not provide the functional and energetic requirements for this interaction. To determine the molecular basis of SpeC recognition of Vβ2.1, we performed alanine-scanning mutagenesis involving all SpeC residues that contact Vβ2.1. Subsequently, the wild-type and mutant SpeC proteins were subjected to a comprehensive battery of functional and energetic analyses. In this integrative approach, stimulatory capacities of bulk primary T cell populations, activation of specific Vβ subsets, binding parameters to soluble Vβ2.1, as well as quantitative measures of the activation of engineered Vβ2.1$^+$ Jurkat T cells were derived for each protein (Table I).

Using primary human T cells, we have shown that SpeC residues Tyr^{15} and Arg^{181} are of critical importance for the recognition of virtually all human T cells (Table I and Fig. 1*B*). Residues Phe^{75} and Leu^{78}, when mutated to alanine, resulted in the stimulation of only a subpopulation of primary Vβ2$^+$ T cells. The remaining SpeC mutants showed insignificant effects on proliferation indexes for the complete T cell repertoire.

To determine the energetic contributions of each of the SpeC residues that comprise the molecular interface with Vβ2.1, we performed SPR analysis. The wild-type and each of the SpeC mutants were individually immobilized and serial dilutions of soluble

Vβ2.1, with a maximum concentration of 100 μM, were injected over each surface. As for other wild-type SAg-TCR interactions, the SpeC-Vβ2.1 complex has an affinity in the midmicromolar range (K_D = 13 μM; Table I, Fig. 2*A*). Two SpeC mutants (T18A and N79A) exhibited ~2-fold reduced binding to Vβ2.1 compared with the wild type (Fig. 2*B*). Several of the SpeC mutants (T20A, R45A, Y49A, and T180A) exhibited no significant change in binding affinity relative to the wild type (Fig. 2*C*). The remaining SpeC alanine mutants (Y15A, I19A, F75A, L78A, E178A, and R181A) had no detectable binding to Vβ2.1, at least at concentrations as high as 100 μM (Fig. 2*D*).

To ascertain the Vβ2.1-specific functional contributions of each SpeC residue, we engineered Jurkat T cells to exclusively express Vβ2.1 receptors (eJRT3-2.1) and activated these cells with wild-type SpeC and each of the mutants. Alanine mutations at four of the critical residues (Tyr^{15}, Phe^{75}, Leu^{78}, and Arg^{181}) did not produce significant quantities of IL-2 from eJRT3-2.1, while mutants at positions Ile^{19}, Tyr^{49}, and Glu^{178} produced reduced amounts (Fig. 3*B*). The ability of both I19A and E178A to activate eJRT3-2.1 (Fig. 3*B*), despite our inability to detect binding of these mutants to Vβ2.1 (Table I), may simply be due to a sensitivity limitation of the Biacore experiments. Stabilizing forces present in the cell-based assays such as TCR α-chain/MHC class II β-chain interactions (15, 16), that are lacking in the affinity measurements which use purified TCR β-chain, could account for these discrepancies. As well, the mutants with low affinities for the TCR β-chain may still induce transient TCR oligomerization, and thus lead to partial signaling. The two mutants with relatively minor (i.e., ~2-fold) reductions in binding to Vβ2.1 (Thr^{18} and Asn^{79}) and the remaining mutants with no apparent change in binding affinity to Vβ2.1 (Thr^{20}, Arg^{45}, Tyr^{49}, and Thr^{180}) also displayed slight reductions in IL-2 production from the engineered Jurkat T cells (Fig. 3*B*). Based on the collective data, including the proliferation indexes, activation of primary V$\beta2^+$ T cells, affinity measurements for soluble Vβ2.1, and activation of Vβ2.1-specific Jurkat T cells, we conclude that the remaining residues Thr^{20}, Arg^{45}, Tyr^{49}, and Thr^{180} play little to no role for the activation of V$\beta2^+$ T cells. However, residues that were critical for the specific recognition of the human Vβ2.1 allele used here also included Phe^{75} and Leu^{78}, while Ile^{19} and Glu^{178} had significant, but not critical, effects (Table I and Fig. 3*B*).

The binding affinities of the various SpeC mutants to soluble Vβ2.1 were correlated with the activation experiments using the eJRT3-2.1 cells. The energetic and functional contributions of individual SpeC residues to the interaction with Vβ2.1 have been mapped to the surface of SpeC (Fig. 4*B*). The critical binding residues (shown in red; Tyr^{15}, Phe^{75}, Leu^{78}, and Arg^{181}), as well as those lacking detectable binding to Vβ2.1 but that still activate eJRT3-2.1 (shown in orange; Ile^{19} and Glu^{178}), all coalescence in the center of the binding cleft. The intermediate resides demonstrating minor reductions in affinity (shown in yellow; Thr^{18} and Asn^{79}) are located on opposite poles of the critical residues, and the neutral residues showing no differences in affinity (shown in green; Thr^{20}, Arg^{45}, Tyr^{49} and Thr^{180}) occur in the periphery of the binding cleft.

The term "hot spot" is used to describe amino acid residues within a protein-protein interface that contribute significantly to the binding energy (20). Hot spot residues typically have a nonrandom distribution within a molecular interface, but are often clustered into "hot regions" (38, 39). The six residues identified here as important for Vβ2.1 recognition fit the criteria of a single, well-defined hot region located within the center of the interface. In this way, the SpeC functional epitope is similar to many protein-protein interactions, where most of the energetically important residues were also clustered in the center of the interface. These critical residues in the centralized hot region on the SpeC molecular surface form a high-energy binding pocket that accommodates the tip of the CDR2 loop and makes several specific hydrogen bonds and van der Waals interactions with the side chain of the inserted residue Ser^{52a} (Fig. 4*C*). Because essentially all of the binding energy is centered on the engagement of the CDR2 loop in this hot region, and the SpeC surface that binds the loop is highly concave (at least in relation to most protein-protein interfaces), it is possible that small molecules could be developed that inhibit the SpeC-Vβ2.1 interaction, and thus, could serve as potential therapeutics of SpeC-mediated disease.

The TCR CDR3 loops are the most variable regions of the TCR, generated through random rearrangement of the various TCR gene segments (40). These loops also make the most contacts with the antigenic peptide and are responsible for different peptide specificities between different Vβs. Of bacterial SAgs, only the *Mycoplasma arthritidis* mitogen has been shown to be functionally dependent on distinct residues of the CDR3 loop for T cell activation (41). The $O^{\partial 1}$ atom of SpeC residue Asn^{79} was shown crystallographically to form hydrogen bonds with main chain atoms of the Vβ2.1 CDR3 loop (Gly^{97} and Ser^{98}), suggesting that SpeC may also rely on the CDR3 loop structure for TCR binding (1). Wild-type SpeC, however, activated practically all primary V$\beta2^+$ T cells, an unexpected result if indeed CDR3 contacts were functionally relevant. Although the N79A mutant had wild-type activity for activation of V$\beta2^+$ T cells (Fig. 1*B*), it did exhibit minor reductions in binding affinity to soluble Vβ2.1 (Table I) and IL-2 production by eJRT3-2.1 cells (Fig. 3*B*). This residue most likely influences CDR1, and not CDR3, loop interactions and based on the collective data, we conclude that CDR3 plays no significant role in SpeC engagement of Vβ2.1.

SpeC has been reported to target T cells expressing human Vβs 2, 3, 4, 12, and 15, with the majority being V$\beta2^+$ T cells (31). Only two Vβ families contain the CDR2 Ser^{52a} insertion, Vβ2 and Vβ4 (9), and SpeC has also been reported to activate both of these Vβs. However, V$\beta2^+$ T cells are activated ~15-fold higher compared with V$\beta4^+$ T cells (31). Differences between the reactivity for these two Vβs have been proposed to be due to a second unique residue insertion (Phe^{27a}), found only in the CDR1 loop of *Vβ2* alleles. Although Phe^{27a} is not contacted by SpeC, this insertion induces an altered conformation of the CDR1 loop such that it positions the loop to make contacts with SpeC (1). The remaining SpeC-targeted Vβ domains do not contain either of these CDR insertions and although the precise architecture by how SpeC may engage these TCRs is unknown, both Tyr^{15} and Arg^{181} also appear critical for activation of T cells expressing these Vβ domains. It should be noted, however, that significantly lower activation levels of V$\beta3^+$, V$\beta12^+$, and V$\beta15^+$, even in comparison to V$\beta4.1^+$, T cells were reported (31).

SpeC residues that contact CDR1 include Arg^{45}, Tyr^{49}, Leu^{78}, and Asn^{79}, and although only L78A had a dramatic phenotype for the interaction with Vβ2.1, the collective binding contribution from each of these likely function to stabilize the overall interaction, accounting for the preferred interaction with Vβ2 over Vβ4. The results of our integrative approach to mapping the SpeC-Vβ2.1 interface support the previously proposed hypothesis that Vβ binding by SpeC is critically dependent on the CDR2 insertion, while the CDR1 insertion is neither critical nor sufficient, but instead augments Vβ binding and T cell activation.

Our results also indicate that of the residues important for engagement of Vβ2.1, not all are critical for binding other Vβ domains, such that differences in binding may occur even within an individual Vβ family. Activation of eJRT3-2.1 and the binding

data are entirely specific for the Vβ2.1 chain used here. Human Vβ families are grouped based on >75% nucleotide identity, and in humans the Vβ2 family has two main isoforms: Vβ2.1 and Vβ2.2 (9). Although residues Phe^{75} and Leu^{78} were critical for binding to soluble Vβ2.1 and for activation of eJRT-2.1, the majority of primary V$\beta2^+$ T cells were still activated by mutants F75A and L78A, while a subset of V$\beta2^+$ T cells were clearly not activated for both of these mutants (Fig. 1*B*). This subset of nonactivated T cells likely represents cells expressing specifically the Vβ2.1 TCRs, whereas the activated V$\beta2^+$ T cells likely represent Vβ2.2 TCRs.

Other than differences in the hypervariable CDR3 loops (which we have shown plays a minor, if any, role in SpeC binding), the human Vβ2.1 subfamily contains seven alleles that collectively vary at positions Arg^{10}, Gln^{41}, Leu^{45}, Met^{46}, and Ser^{52a} (numbering is according to the Vβ2.1 used here). Of these, only Ser^{52a} makes contacts with SpeC. One Vβ2.1 chain contains a Cys at position 52a, rather than a Ser found in the other six alleles. It is not known whether the Cys^{52a} Vβ2.1 allele can be activated by SpeC, but it is possible that the Cys^{52a} S^{γ} could functionally replace Ser^{52a} O^{γ} to hydrogen bond between the side chains of Tyr^{15} and Arg^{181} of SpeC (Fig. 4*C*). The Vβ2.2 subfamily varies from Vβ2.1 at additional positions, including Arg^{10}, Lys^{20}, Phe^{38}, Pro^{39}, Lys^{53}, Ala^{54}, Glu^{61}, Leu^{66}, Ala^{70}, Ser^{71}, Leu^{74}, and Thr^{76}. Of these, intermolecular contacts likely occur (based on the Vβ2.1-SpeC crystal structure) only at positions Lys^{53} and Ala^{54}. Although neither of these residues makes direct contacts with SpeC residues Phe^{75} or Leu^{78} (which contact the CDR2 loop residues Gly^{52} and Ser^{52a}), all four of these Vβ residues (Gly^{52}, Ser^{52a}, Lys^{53} and Ala^{54}) are within the CDR2 loop. Vβ2.2 contains a Val at position 54, a relatively conservative change, while a Glu is positioned at position 53. This Lys→Glu substitution may be responsible for the V$\beta2.2^+$ T cell activation observed in response to the F75A and L78A SpeC mutants through an alteration in the CDR2 loop, likely centered at the flexible Gly^{51} position. This hypothesis, however, remains to be formally tested.

Comparison of the Vβ2.1 structure in complex with SpeC (1), with that from a different Vβ2.1 chain from an autoimmune TCR-p/MHC complex (42), indicates that the CDR2 loop exists in significantly different conformations when bound to either agonist p/MHC or to SpeC (Fig. 4*D*). The side chains of residues Tyr^{15} and Arg^{181} both sandwich the Ser^{52a} O^{γ} atom through a pair of hydrogen bonds. Assuming movement of CDR2 by engagement with SpeC relative to the autoimmune Vβ2.1 TCR, the C^{α} and O^{γ} atoms of Ser^{52a} undergo movements of 4.7 and 5.3 Å, respectively, away from the SpeC surface (Fig. 4*D*). This observation is also consistent with plasticity of the CDR2 loop in mouse Vβ8.2 upon engagement with SEC3 (43). Furthermore, previous work using random mutagenesis targeting mouse Vβ8.2 CDR2 for affinity maturation binding to SEC3 failed to alter two glycine residues (position 51 and 53) (44), presumably important for flexibility. The flexibility of the CDR2 loop also plays both energetic and functional roles in negative cooperativity in the mouse Vβ8.2-SEC3 interaction (43, 45). Thus, despite the mechanistic diversity with which SAgs engage their TCR Vβ domain ligands, CDR2 plasticity may play a common and important functional role.

Although SAgs are defined by their ability to activate T cells in a Vβ-specific manner (8), our data indicates that fine specificity may exist for SAg targets even within an individual Vβ family, and although some SAgs such as SEB and SEC3 appear to have evolved to target TCR Vβs through mechanisms that may be more dependent on the conformation of the Vβ CDR loops, other SAgs such as SpeC appear to have evolved to target highly specific features of Vβ CDR loops. When combined with other relevant data, such as the CDR3-dependent binding of *Mycoplasma arthritidis* mitogen (41), and the apparent Vα specificity of SEH (46), SAgs have likely evolved to engage their TCR ligands through a variety of diverse mechanisms. The integrative approach to mapping SAg-TCR interactions (structurally, energetically, and functionally) provides comprehensive descriptions of these engagement mechanisms and affords a greater understanding of SAg-TCR selectivity and cross-reactivity, thereby providing a foundation for a more rationalized approach to SAg antagonism.

Disclosures

The authors have no financial conflict of interest.

References

1. Sundberg, E. J., H. Li, A. S. Llera, J. K. McCormick, J. Tormo, P. M. Schlievert, K. Karjalainen, and R. A. Mariuzza. 2002. Structures of two streptococcal superantigens bound to TCR β chains reveal diversity in the architecture of T cell signaling complexes. *Structure* 10: 687–699.
2. Jardetzky, T. S., J. H. Brown, J. C. Gorga, L. J. Stern, R. G. Urban, Y. I. Chi, C. Stauffacher, J. L. Strominger, and D. C. Wiley. 1994. Three-dimensional structure of a human class II histocompatibility molecule complexed with superantigen. *Nature* 368: 711–718.
3. Kim, J., R. G. Urban, J. L. Strominger, and D. C. Wiley. 1994. Toxic shock syndrome toxin-1 complexed with a class II major histocompatibility molecule HLA-DR1. *Science* 266: 1870–1874.
4. Petersson, K., M. Hakansson, H. Nilsson, G. Forsberg, L. A. Svensson, A. Liljas, and B. Walse. 2001. Crystal structure of a superantigen bound to MHC class II displays zinc and peptide dependence. *EMBO J.* 20: 3306–3312.
5. Li, Y., H. Li, N. Dimasi, J. K. McCormick, R. Martin, P. Schuck, P. M. Schlievert, and R. A. Mariuzza. 2001. Crystal structure of a superantigen bound to the high-affinity, zinc-dependent site on MHC class II. *Immunity* 14: 93–104.
6. Li, H., A. Llera, D. Tsuchiya, L. Leder, X. Ysern, P. M. Schlievert, K. Karjalainen, and R. A. Mariuzza. 1998. Three-dimensional structure of the complex between a T cell receptor β chain and the superantigen staphylococcal enterotoxin B. *Immunity* 9: 807–816.
7. Zhao, Y., Z. Li, S. J. Drozd, Y. Guo, W. Mourad, and H. Li. 2004. Crystal structure of *Mycoplasma arthritidis* mitogen complexed with HLA-DR1 reveals a novel superantigen fold and a dimerized superantigen-MHC complex. *Structure* 12: 277–288.
8. Marrack, P., and J. Kappler. 1990. The staphylococcal enterotoxins and their relatives. *Science* 248: 705–711.
9. Arden, B., S. P. Clark, D. Kabelitz, and T. W. Mak. 1995. Human T-cell receptor variable gene segment families. *Immunogenetics* 42: 455–500.
10. Wei, S., P. Charmley, M. A. Robinson, and P. Concannon. 1994. The extent of the human germline T-cell receptor Vβ gene segment repertoire. *Immunogenetics* 40: 27–36.
11. McCormick, J. K., J. M. Yarwood, and P. M. Schlievert. 2001. Toxic shock syndrome and bacterial superantigens: an update. *Annu. Rev. Microbiol.* 55: 77–104.
12. Wucherpfennig, K. W. 2001. Mechanisms for the induction of autoimmunity by infectious agents. *J. Clin. Invest.* 108: 1097–1104.
13. Lavoie, P. M., H. McGrath, N. H. Shoukry, P. A. Cazenave, R. P. Sekaly, and J. Thibodeau. 2001. Quantitative relationship between MHC class II-superantigen complexes and the balance of T cell activation versus death. *J. Immunol.* 166: 7229–7237.
14. Fields, B. A., E. L. Malchiodi, H. Li, X. Ysern, C. V. Stauffacher, P. M. Schlievert, K. Karjalainen, and R. A. Mariuzza. 1996. Crystal structure of a T-cell receptor β-chain complexed with a superantigen. *Nature* 384: 188–192.
15. Andersen, P. S., P. M. Lavoie, R. P. Sekaly, H. Churchill, D. M. Kranz, P. M. Schlievert, K. Karjalainen, and R. A. Mariuzza. 1999. Role of the T cell receptor α chain in stabilizing TCR-superantigen-MHC class II complexes. *Immunity* 10: 473–483.
16. Andersen, P. S., P. Schuck, E. J. Sundberg, C. Geisler, K. Karjalainen, and R. A. Mariuzza. 2002. Quantifying the energetics of cooperativity in a ternary protein complex. *Biochemistry* 41: 5177–5184.
17. Proft, T., and J. D. Fraser. 2003. Bacterial superantigens. *Clin. Exp. Immunol.* 133: 299–306.
18. Li, H., A. Llera, E. L. Malchiodi, and R. A. Mariuzza. 1999. The structural basis of T cell activation by superantigens. *Annu. Rev. Immunol.* 17: 435–466.
19. Bogan, A. A., and K. S. Thorn. 1998. Anatomy of hot spots in protein interfaces. *J. Mol. Biol.* 280: 1–9.
20. DeLano, W. L. 2002. Unraveling hot spots in binding interfaces: progress and challenges. *Curr. Opin. Struct. Biol.* 12: 14–20.
21. Clackson, T., and J. A. Wells. 1995. A hot spot of binding energy in a hormone-receptor interface. *Science* 267: 383–386.
22. Guerois, R., J. E. Nielsen, and L. Serrano. 2002. Predicting changes in the stability of proteins and protein complexes: a study of more than 1000 mutations. *J. Mol. Biol.* 320: 369–387.
23. Huo, S., I. Massova, and P. A. Kollman. 2002. Computational alanine scanning of the 1:1 human growth hormone-receptor complex. *J. Comput. Chem.* 23: 15–27.

24. Kortemme, T., and D. Baker. 2002. A simple physical model for binding energy hot spots in protein-protein complexes. *Proc. Natl. Acad. Sci. USA* 99: 14116–14121.
25. Massova, I., and P. A. Kollman. 1999. Computational alanine scanning to probe protein-protein interactions: a novel approach to evaluate binding free energies. *J. Am. Chem. Soc.* 121: 8133–8143.
26. Sharp, K. A. 1998. Calculation of HyHel10-lysozyme binding free energy changes: effect of ten point mutations. *Proteins* 33: 39–48.
27. Sambrook, J., and D. W. Russell. 2001. *Molecular Cloning: A Laboratory Manual.* Cold Spring Harbor Laboratory Press, Cold Spring Harbor.
28. Kapust, R. B., J. Tozser, J. D. Fox, D. E. Anderson, S. Cherry, T. D. Copeland, and D. S. Waugh. 2001. Tobacco etch virus protease: mechanism of autolysis and rational design of stable mutants with wild-type catalytic proficiency. *Protein Eng.* 14: 993–1000.
29. McCormick, J. K., T. J. Tripp, S. B. Olmsted, Y. V. Matsuka, P. J. Gahr, D. H. Ohlendorf, and P. M. Schlievert. 2000. Development of streptococcal pyrogenic exotoxin C vaccine toxoids that are protective in the rabbit model of toxic shock syndrome. *J. Immunol.* 165: 2306–2312.
30. Goshorn, S. C., and P. M. Schlievert. 1988. Nucleotide sequence of streptococcal pyrogenic exotoxin type C. *Infect. Immun.* 56: 2518–2520.
31. Li, P. L., R. E. Tiedemann, S. L. Moffat, and J. D. Fraser. 1997. The superantigen streptococcal pyrogenic exotoxin C (SPE-C) exhibits a novel mode of action. *J. Exp. Med.* 186: 375–383.
32. Weiss, A., and J. D. Stobo. 1984. Requirement for the coexpression of T3 and the T cell antigen receptor on a malignant human T cell line. *J. Exp. Med.* 160: 1284–1299.
33. Ohashi, P., T. Mak, P. Van den Elsen, Y. Yanagi, Y. Yoshikai, A. Calan, C. Terhorst, J. Stobo, and A. Weiss. 1985. Reconstitution of an active surface T3/T-cell antigen receptor by DNA transfer. *Nature* 316: 606–609.
34. Strathdee, C., M. McLeod, and J. Hall. 1999. Efficient control of tetracycline-responsive gene expression from an autoregulated bi-directional expression vector. *Gene* 229: 21–29.
35. Wells, J. A. 1991. Systematic mutational analyses of protein-protein interfaces. *Methods Enzymol.* 202: 390–411.
36. Reddy, M., E. Eirikis, C. Davis, H. M. Davis, and U. Prabhakar. 2004. Comparative analysis of lymphocyte activation marker expression and cytokine secretion profile in stimulated human peripheral blood mononuclear cell cultures: an in vitro model to monitor cellular immune function. *J. Immunol. Methods* 293: 127–142.
37. Sundberg, E. J., Y. Li, and R. A. Mariuzza. 2002. So many ways of getting in the way: diversity in the molecular architecture of superantigen-dependent T-cell signaling complexes. *Curr. Opin. Immunol.* 14: 36–44.
38. Reichmann, D., O. Rahat, S. Albeck, R. Meged, O. Dym, and G. Schreiber. 2005. The modular architecture of protein-protein binding interfaces. *Proc. Natl. Acad. Sci. USA* 102: 57–62.
39. Keskin, O., B. Ma, and R. Nussinov. 2005. Hot regions in protein-protein interactions: the organization and contribution of structurally conserved hot spot residues. *J. Mol. Biol.* 345: 1281–1294.
40. Davis, M. M., and P. J. Bjorkman. 1988. T-cell antigen receptor genes and T-cell recognition. *Nature* 334: 395–402.
41. Hodtsev, A. S., Y. Choi, E. Spanopoulou, and D. N. Posnett. 1998. Mycoplasma superantigen is a CDR3-dependent ligand for the T cell antigen receptor. *J. Exp. Med.* 187: 319–327.
42. Hahn, M., M. J. Nicholson, J. Pyrdol, and K. W. Wucherpfennig. 2005. Unconventional topology of self peptide-major histocompatibility complex binding by a human autoimmune T cell receptor. *Nat. Immunol.* 6: 490–496.
43. Cho, S., C. P. Swaminathan, J. Yang, M. C. Kerzic, R. Guan, M. C. Kieke, D. M. Kranz, R. A. Mariuzza, and E. J. Sundberg. 2005. Structural basis of affinity maturation and intramolecular cooperativity in a protein-protein interaction. *Structure* 13: 1775–1787.
44. Kieke, M. C., E. Sundberg, E. V. Shusta, R. A. Mariuzza, K. D. Wittrup, and D. M. Kranz. 2001. High affinity T cell receptors from yeast display libraries block T cell activation by superantigens. *J. Mol. Biol.* 307: 1305–1315.
45. Yang, J., C. P. Swaminathan, Y. Huang, R. Guan, S. Cho, M. C. Kieke, D. M. Kranz, R. A. Mariuzza, and E. J. Sundberg. 2003. Dissecting cooperative and additive binding energetics in the affinity maturation pathway of a protein-protein interface. *J. Biol. Chem.* 278: 50412–50421.
46. Petersson, K., H. Pettersson, N. J. Skartved, B. Walse, and G. Forsberg. 2003. Staphylococcal enterotoxin H induces Vα-specific expansion of T cells. *J. Immunol.* 170: 4148–4154.